MÖSSBAUER EFFECT STUDIES OF FINE ARTS

B. Keisch

MÖSSBAUER EFFECT STUDIES OF FINE ARTS

B. KEISCH

National Gallery of Art Research Project, Carnegie-Mellon Institute of Research, 4400 Fifth Avenue, Pittsburgh, Pennsylvania 15213 USA

Résumé. — Dans le but de démontrer l'emploi de la Spectroscopie à Effet Mössbauer dans le domaine des beaux-arts, on a passé en revue les pigments contenant du fer, on a conçu et construit un détecteur à rétrodiffusion et l'on a étudié des statuettes en terre cuite. Ces résultats démontrent une haute possibilité de classifier les pigments contenant des oxydes de fer et utilisés par les artistes afin d'aider à leur identification ; ils montrent aussi que l'on peut obtenir de façon efficace et sans les endommager des spectres d'œuvres d'art et que l'on peut résoudre certains genres de problèmes qui ont rapport aux différences entre statuettes en terre cuite.

Abstract. — In an effort to demonstrate the application of Mössbauer Effect Spectroscopy in the field of Fine Arts, a survey of iron-bearing pigments was undertaken, a back-scattering detector was designed and constructed, and terra-cotta statuary was studied. These results show that there is great potential for classifying artists' pigments that contain iron oxides as an aid to identification, that spectra can be obtained on works of art efficiently and harmlessly, and that certain types of problems can be solved regarding differences in terra-cotta statues.

1. **Introduction.** — Because of the common occurrence of iron compounds in rocks of the earth's crust and the variety of color exhibited by these compounds, iron is an important constituent, by design and by accident, in many works of art. One method, which can be made completely non-destructive, to study the properties of iron compounds and to identify them is the use of Mössbauer Effect (ME) Spectroscopy. While most ME data have been collected in a transmission mode, which requires either thin samples or some sample preparation to achieve *thinness*, the collection of data by means of scattering allows one to achieve the same results with no sample preparation whatsoever. That is, provided the compound to be studied lies at or very near the surface of the material in which the compound occurs.

In the study of works of art the latter proviso is usually satisfied since iron compounds occur as pigments at the esthetic surface of a painting (often covered by only a thin layer of varnish) or are homogeneously distributed throughout the matrix of statuary material, such as terracotta.

A list of iron pigments and compounds, and iron-bearing materials used by artists is given in Table I. We have studied many of these with varying degrees of thoroughness in a survey seeking possible applications of this analytical tool to art identification.

2. **Mössbauer effect by transmission.** — 2.1 EXPERIMENTAL ARRANGEMENT. — Since we wished to begin our studies of pigments using samples of the *pure* material, the transmission mode was used with no particularly novel techniques.

TABLE I

A list of iron-bearing art materials

I. Pigments
- Yellow ochre
- Raw sienna
- Burnt sienna
- Raw umber
- Burnt umber
- Red iron oxide (variety of synonyms), red ochre, mars red, synthetic and natural
- Black iron oxide, synthetic and natural
- Synthetic yellow oxides, mars orange, mars yellow
- Brown iron oxides
- Green earth
- Prussian blue
- Van Dyke Brown

II. Other materials
- Terracotta
- Pottery (various colors)

The source employed was a cobaltous oxide source (*) containing approximately 10 millicuries of Co-57. The spectrometer was a Nuclear Science Instruments (Duquesne, Pa.) model MM-60 coupled to a Northern Scientific (Middletown, Wisc.) model NS-600, 1 024-channel pulse height analyser. An ORTEC (Oak Ridge, Tenn.) model 485 amplifier and

(*) Obtained from New England Nuclear Corporation, Boston, Massachusetts.

model 109 PC preamplifier was used in conjunction with a home-made 90 % krypton-10 % methane-filled proportional counter. The high voltage supply was a Fluke (Seattle, Wash.) model 412B. The velocity of the system was calibrated with natural iron foil as an absorber. All spectra were obtained at room temperature (~ 22 °C).

Powdered samples were mounted between two 22 mm diameter acrylic discs with a total thickness of 2 mm. The sample, typically weighing approximately 50-100 mg, was lightly compressed to a thickness of 1 mm between the discs and confined by a rim on one of them. The assembly was held together by self-adhesive tape applied around its perimeter.

The data obtained for all of the spectra obtained by transmission were processed by computer (IBM 360/67) and the fitted plots were also generated by the computer. The particular program used [1] locates peaks and adjusts peak height and width in an iterative process to obtain a least squares fit, but the user must decide on the number of peaks to be located. The user may also initially choose the locations, heights, and/or widths of any or all of the peaks and may choose to restrict the fit to equal peak widths. It is not possible to fit two peaks in the same position even if they are each a part of two different superimposed spectra.

2.2 SURVEY OF MATERIALS BY ME (TRANSMISSION). — 2.2.1 « *Red iron oxides* ». — Red iron oxide pigments, chemically α-Fe_2O_3, may be natural or produced synthetically. Natural material may be merely ground and washed or, in addition may be heated. Synthetic material may be produced by direct precipitation, by calcination of ferrous sulfate (with or without the presence of other materials such as $Ca(OH)_2$) or by calcination of synthetic or natural yellow oxides. The last may be termed *burnt* ochre or sienna and are discussed later. Mixtures of synthetic and natural material may also occur.

We obtained ME spectra for 15 different samples as listed in Table II with their source and/or method of production as well as the manufacturers claimed Fe_2O_3 content where known.

All of these exhibit very similar 6-peak spectra (magnetic hyperfine splitting) of which figures 1*a* and 1*b* are examples. Figure 1*a* is almost an ideal spectrum for the compound α-Fe_2O_3, while Figure 1*b*, like many of the others, shows peak broadening and peak areas that are not in the theoretical ratios 3 : 2 : 1 : 1 : 2 : 3. These *non-ideal* spectra may be due to a particle-size phenomenon (see Section 2.3). Samples prepared from natural material, B-52, B-49, B-45, B-342, B-326 and B-368, should be compared with the natural reds in paragraph 2.2.5 below.

TABLE II

Red iron oxides analysed ([1])

Sample No.	Name	Mfg. or Source	Description	% Fe_2O_3
—	—	—	—	—
B-52	*Spanish red oxide*	RC	natural, possibly calcined	(88 % Fe_2O_3)
B-43	Red oxide	RC	« chemical by-product »	(95 % Fe_2O_3)
B-49	Red iron oxide	W	natural	(74-78 % Fe_2O_3)
B-47	*Venetian red*	RC	calcined mixture of ferrous sulfate and calcium hydroxide yielding Fe_2O_3 + $CaSO_4$	(40 % Fe_2O_3)
B-50	*Kroma red oxide*	W	direct precipitation	(96 % Fe_2O_3)
B-55	*Pure indian red*	RC	calcined ferrous sulfate	(97 % Fe_2O_3)
B-45	*Super aetna crimson red*	RC	natural possibly calcined	(82 % Fe_2O_3)
B-48	Red iron oxide	W	calcined ferrous sulfate	(99 % Fe_2O_3)
B-342	Natural oxide	Italian		
B-326	Terra pozzouli	Italian	natural	
B-39	Red oxide	Source unknown	type unknown	
B-368	Red iron oxide marron shade	RC	natural, possibly calcined and/or mixed with synthetic material	(89 % Fe_2O_3)
B-374	Red iron oxide	RC	chemically precipitated	(98 % Fe_2O_3)
B-376	Metallic brown iron oxide	RC	calcined natural	(97 % Fe_2O_3)
B-375	Red iron oxide	RC	calcined ferrous sulfate	(98 % Fe_2O_3)

([1]) Underlined names are manufacturer's designations.
RC = Reichard-Coulston, Inc.
W = Williams (Minerals, Pigments, and Metals Div., Chas. Pfizer & Co.).

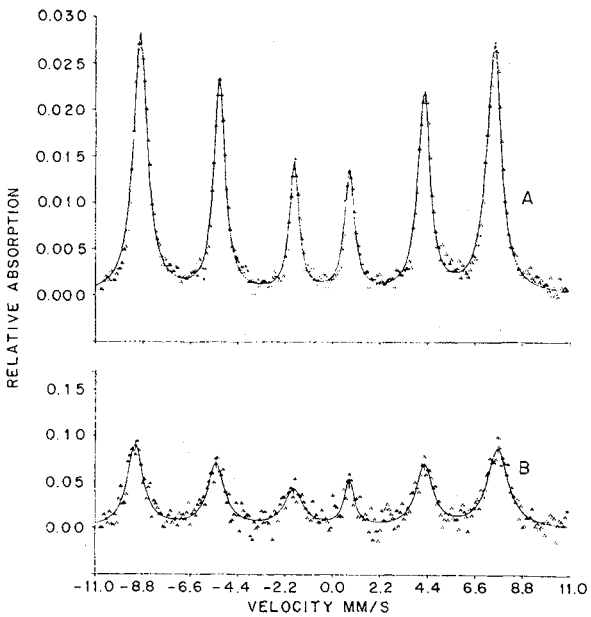

FIG. 1. — *a*) Red iron oxide B-374. *b*) Red oxide B-43.

2.2.2 *Black iron oxide.* — Black iron oxide, a ferro-ferric oxide having an empirical formula Fe_3O_4, is not commonly used as an artist's pigment and is not listed by Harley [2] or Gettens [3]. However, it is available as a modern pigment and while frequently shunned in favor of one of the carbon blacks, it is used alone or more commonly in a mixture with carbon black or in the preparation of synthetic brown oxides.

Figure 2 is the ME spectra obtained on a sample from Reichard-Coulston containing 93 % iron oxide (sample number B-367). There are actually twelve

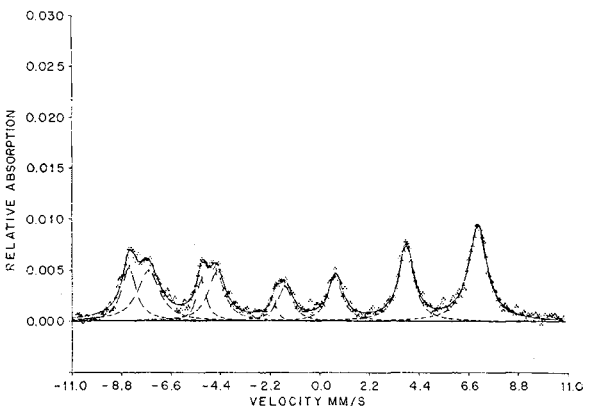

FIG. 2. — Black iron oxide.

peaks but only nine are resolved here. It is noteworthy that the relative intensities of the two superimposed 6-peak spectra are reversed from published data [4]. This might indicate that the material is partially oxidized and not pure Fe_3O_4.

2.2.3 *Yellow iron oxides. Synthetic.* — Yellow iron oxide is the hydrate of Fe_2O_3. The preferred empirical formula is FeOOH. This compound has been reported in 4 structural modifications [5], the most common of which is α-FeOOH or goethite. The color may vary from *light lemon* through *dark orange.*

Synthetic yellow oxide is produced by chemical precipitation and is goethite. Figure 3*a* is the ME spectrum we obtained from a sample of Reichard-Coulston's *Irox yellow* (sample number B-57) containing 87 % Fe_2O_3 (theoretical amount for pure α-FeOOH = 89.9 %). A synthetic lemon yellow oxide (sample number B-103) yielded a similar spectrum.

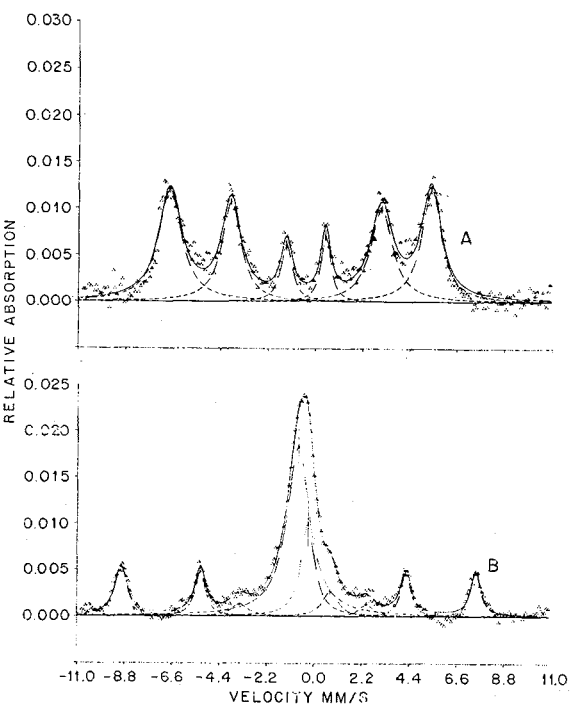

FIG. 3. — *a*) Irox yellow B-57. *b*) Mars orange B-106.

Figure 3*b* is the spectrum obtained from a sample of a synthetic *yellow* oxide called *Mars Orange* (sample number B-106), once known as an *artificial ochre.* Actually, although it was included in this group because of its color, it is a sample of hematite (α-Fe_2O_3) with very small crystallites.

Calcination of the yellow oxides results in the red oxide α-Fe_2O_3.

2.2.4 *Natural yellow oxides. Ochre, sienna and umber.* — Yellow ochre, raw sienna, and raw umber are naturally occurring yellow iron-bearing earths containing varying amounts of silica and alumina that owe their color principally to α-FeOOH. Umber also contains varying amounts of manganese dioxide, which imparts a greenish-brown color to the pigment. Ochres are considered to be those iron-bearing earths that contain between approximately 15 to 40 % Fe_2O_3 (based on dry weight) while siennas contain more than 40 % Fe_2O_3 [6], but the ready distinction between ochre and sienna is not easy. It has been said

TABLE III

Natural yellow oxides analysed

Sample Number	Name	Source or Mfg.	Description	ME type [1]
B-87	Yellow ochre	Northampton Co., Penna.		I
B-19	Yellow ochre	SOF [2]	Screened	I
B-22	Yellow ochre	SOF	« Micronized »	I
B-21	Yellow ochre	SOF	—	I
B-84	Yellow ochre	French		I
B-415	Yellow ochre	Williams		II
B-82	Ochre	Farmers Museum, Cooperstown, N. Y.	Old can (late 19th cen.)	II
B-26	Raw sienna	Reichard-Coulston	Italian import 70 % Fe_2O_3	I
B-27	Raw sienna	Reichard-Coulston	Domestic	II
B-414	Raw sienna	Williams		II
B-416	Raw sienna	Williams		II
B-411	Raw sienna	Williams	— 68-73 % Fe_2O_3	II
B-17	Raw sienna			II
B-51	Raw turkey umber	Reichard-Coulston	Cyprus import { 49 % Fe_2O_3, 8 % MnO_2	I
B-28	Raw turkey umber	Lowe Bros., Dayton, Ohio [3]	Cyprus import	I
B-65	Cappagh brown			I

[1] See text.

[2] Society des Ochres de France (Auxerre).

[3] Cappagh brown is an umber-like material (containing manganese) that comes from a particular place in Cork County, Ireland.

that sienna is a special kind of ochre, the best of which occurs near Sienna, Italy, with a greater transparency than most ochres [7].

Table III is a descriptive list of the natural yellow earths from which ME spectra were obtained. These include yellow ochre, raw sienna, and raw umber (although the latter is a brown color, chemically it consists essentially of α-FeOOH like the others).

There are two general types of ME spectra obtained. Type I, shown in figure 4*a* (sample number B-19), appears to exhibit what has been previously described [8] as being evidence of super-paramagnetism and the degree to which this occurs appears to be a function of particle size (see Section 2.3). Type II, shown in figure 4*b*, (sample B-27) is a complicated variation of the 6-peak spectrum for α-FeOOH (Fig. 3*a*) probably exhibiting some superparamagnetism. Some type II samples, B-26 for instance, also show the presence of a small amount of α-Fe_2O_3 as two additional small peaks at velocities of approximately − 9.0 and 7.4 mm/s. Two type I samples of this group, B-28 and B-65, show complete superparamagnetism in that only two central peaks are observed in the spectrum. While this could indicate the presence of β-FeOOH, further study showed that this possibility was not the case (see Section 2.3).

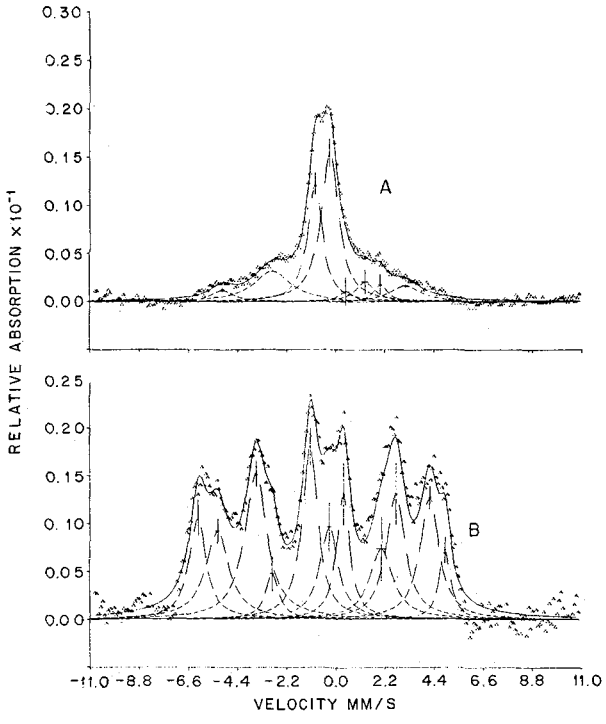

FIG. 4. — *a*) Yellow ochre B-19 (Type I). *b*) Raw sienna B-27 (Type II).

2.2.5 *Red ochre, burnt sienna and burnt umber.* — These natural red or reddish-brown materials are either produced by heating the corresponding yellow or *raw* form, or may be found natural, as in the case of red ochre. In any case, the iron oxide content is mainly in the form of α-Fe_2O_3. Note that in section (2.2.1) above, a number of natural or processed natural red oxides are listed. Chemically the state of the iron is the same. However, those shown in Table IV do not yield the *clean* 6-peak spectrum (hyperfine magnetic splitting) of the pure red oxide.

Two general types of spectra are obtained. Type III shows a prominent central group flanked by a 6-peak spectrum. Figure 5*a* (sample B-54) is an example. The outer peaks seem to correspond to the black oxide (Fe_3O_4) rather than the red and because of the very dark color of this pigment, a burnt umber, one might be inclined to presume that the black oxide predominates, with the central peaks corresponding to superparamagnetism as in the case of the yellow oxides. However, sample B-44, a burnt sienna, yields the same type of spectrum yet is a definite red color (although not *pure* red). Thus these type III spectra may all result from small particle size (see Section 2.3). Note also the similarity between the spectra for sample B-54, a burnt umber, and that for B-106 (Fig. 3*b*), which is a synthetic Mars Orange.

The second type, IV, consists mainly of a 6-peak spectrum corresponding to that obtained for α-Fe_2O_3 except that (*a*) the outermost peaks are note quite so far apart and (*b*) there are smaller peaks in the central part of the spectrum. Figure 5*b* (sample B-23) is a typical example of this type of spectrum. Again

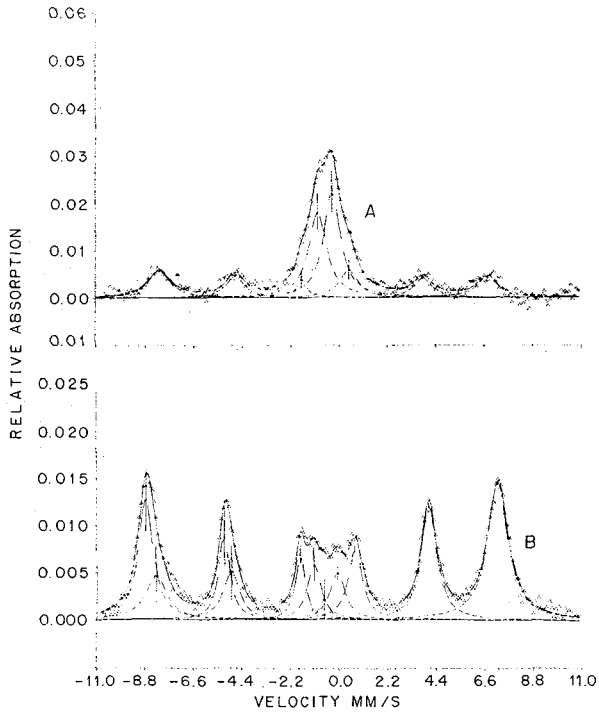

FIG. 5. — *a*) Burnt turkey umber B-54 (Type III). *b*) Red ochre B-23 (Type IV).

TABLE IV

Red ochres and burnt siennas and umbers analysed

Sample Number	Name	Source or Mfg.	Description	Type ME spect.
—	—	—	—	—
B-23	Red ochre	SOF ([1])	Screened	IV
B-24	Red ochre	SOF	« Micronized »	III
B-18	Red ochre	SOF	« Micronized »	IV
B-20	Red ochre	SOF	« Micronized »	IV
B-356	Armenian Bole ([2])	Venice	ca. 1906	IV
B-350	Light red	Winsor & Newton		IV
B-44	Burnt sienna	Reichard-Coulston	Italian import 71 % Fe_2O_3	IV
B-42	Burnt sienna	Lucas Company	—	IV
B-53	Burnt sienna	Reichard-Coulston	Domestic	IV
B-41	Burnt sienna			IV
B-413	Burnt sienna	Williams		IV
B-412	Burnt sienna	Williams		IV
B-40	Burnt sienna			IV
B-373	Burnt turkey umber	Reichard-Coulston	Cyprus import 47 % Fe_2O_3 — 18 % MnO_2	III
B-33	Burnt umber			III
B-54	Burnt turkey umber	Reichard-Coulston	Cyprus import 53 % Fe_2O_3 9 % MnO_2	III

([1]) SOF = Society des Ochres de France (Auxerre).

([2]) Bole is a clay-like material similar to an ochre but softer. This was originally found in Armenia but now elsewhere.

while the possibility exists for presence of some Fe_3O_4 or γ-Fe_2O_3 (maghemite) [9] in these materials, it is likely that we are observing some superparamagnetism. It is quite possible that the two peaks at the extreme left are really only one broadened peak. The prominence of the central peaks varies considerably among the samples in this group. In some cases, for example, B-41, these *extra* peaks are barely discernible.

2.2.6 *Brown pigments containing iron.* — There are several iron-bearing pigments that are brown in color. First, there are calcined naturally occurring materials known in the industry as *metallic brown oxides.* An example, sample B-376, of this has been listed among the red oxides in paragraph (2.2.1) above. The ME spectrum is typical of the red oxide, α-Fe_2O_3, and the color is actually a reddish brown.

The industry also prepares *brown iron oxide* synthetically by mixing various proportions of α-Fe_2O_3 (red), α-FeOOH (yellow), and either carbon black or Fe_3O_4 (black).

When the yellow oxide of the sienna, umber, or ochre type is extremely finely divided, it sometimes appears darker and approaches brown in color. Umbers are particularly good examples of this but they also contain MnO_2, which is black and/or Mn_3O_4, which is red.

Finally, van Dyke Brown (also called Cassel earth or Cologne earth) is a brown peat-like material the color of which is mainly derived from the organic material present. It also contains approximately 1 % iron and is, therefore, included here. ME spectra for these obtained on lightly packed powder approximately 1/4″ thick.

Table V lists brown pigments for which ME spectra were obtained.

The spectra obtained for the synthetic brown mixtures showed, as expected, the presence of the separate pigments making up the mixtures. Also, as expected, the varying proportions of the oxides were evident as the shade of brown varied through reddish, yellowish, and blackish. A typical spectrum, that of sample B-370, is shown in figure 6. This sample

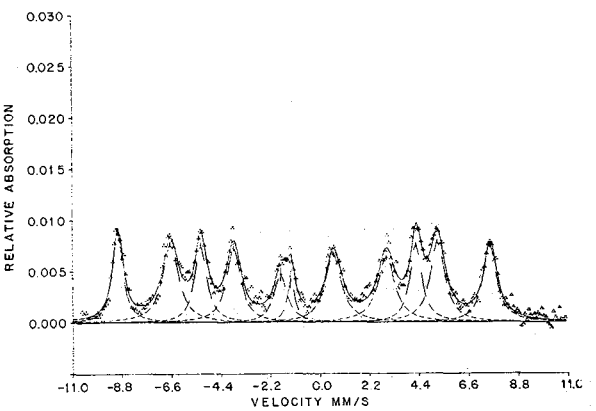

FIG. 6. — Synthetic brown mixture B-370.

undoubtedly contains a large amount of carbon black since it is very dark and not distinctly yellow or red. The difference between sample B-46 and the others is evident in that the width and proportions of the outermost peaks in the spectrum from B-46 is affected by the presence of Fe_3O_4 instead of carbon black.

The spectra obtained from the three van Dyke Brown samples were similar to one another. Two peaks were obtained. For two of the samples, B-419 and B-421, these peaks were located at − 0.92 and − 0.20 mm/s. For the other sample, B-420, the peaks were located at − 0.86 and − 0.03 mm/s. No attempt was made to determine the source of this difference or the nature of the iron compounds involved. The spectra obtained for these three samples are shown in figure 7.

2.2.7 *Green earth (terre-verte).* — Green earth is a centuries-old pigment that is highly variable and complex in composition as is typical of clay minerals. Chiefly it consists of hydrous iron, magnesium, and

TABLE V

Brown iron-bearing pigments analysed

Sample No.	Name	Mfg. or Source	Description
—	—	—	—
B-46	Brown iron oxide	*Williams*	Synthetic mixture of yellow, red, and black oxides
B-369	Brown iron oxide	*Reichard-Coulston*	Synthetic mixture of yellow, red oxides and carbon black
B-371		*Reichard-Coulston*	—
B-372	Brown iron oxide	*Reichard-Coulston*	—
B-370	Brown iron oxide	*Reichard-Coulston*	—
B-420	Van Dyke Brown	*Habich*	Cassel region, Germany (0.8 % Fe)
B-421	Van Dyke Brown	*Urban*	Cassel region, Germany (2 % Fe)
B-419	Van Dyke Brown	*Hawley*	Czechoslovakian import (0.8 % Fe)

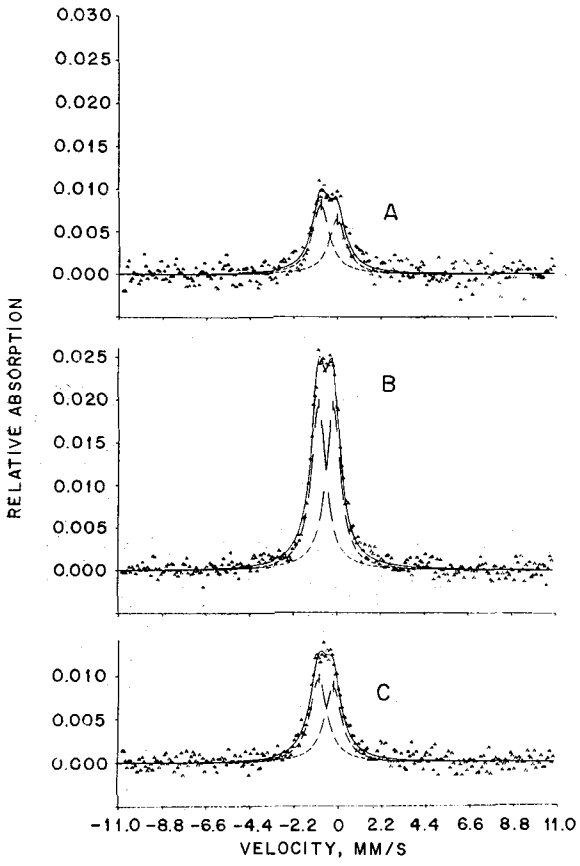

FIG. 7. — Van Dyke Browns : *a*) Cassel, Germany B-420. *b*) Cassel, Germany B-421. *c*) Czechoslovakia B-419.

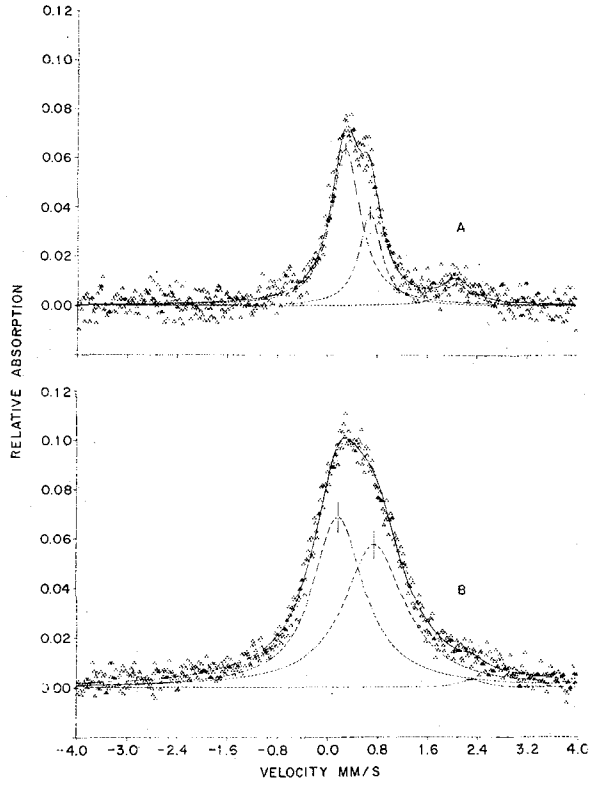

FIG. 8. — *a*) Green earth, Verona, Italy. *b*) *Burnt* green earth.

aluminium-potassium silicates (celadonite and glauconite) [10]. The structure is that of a layered silicate with cations between layers. Part of the iron is in the ferrous state.

ME spectra of green earths indicate that both ferrous and ferric iron are present, chiefly the latter. The ferrous content is variable and related to the color. Upon strong heating, the pigment turns red-brown and the ferrous component in the ME spectrum disappears. *Burnt green-earth* is known and is apparently produced by gentler heating. It has an olive color and a small amount of ferrous component.

The spectrum obtained on a sample of this pigment, shown in figure 8*a*, is that in which the largest amount of ferrous component was observed. The spectrum shown in figure 8*b* is that of a sample of *burnt green earth*. Other samples yielded similar spectra with various proportions of ferrous and ferric components. Experiments are continuing in an attempt to learn more about the variations in this material.

2.2.8 *Prussian blue*. — Prussian blue, technically $Fe_4(Fe[CN]_6)_3$, is a commonly used synthetic pigment in use almost from the time it was first synthesized in 1704. Its permanence is only fair in that it is not entirely lightfast and is sensitive to alkalis. It is believed that light-induced fading might be reversible but the mechanism is not well understood.

We set out to detect a chemical change related to the fading process using the Mössbauer Effect and to this end a film of Prussian blue diluted with titanium white (TiO_2) in an acrylic medium was applied to a 6″ × 3″ × 1/16″ Plexiglas(R) panel. Half of the panel was protected by a covering of aluminum foil and the other half exposed for 500 hours in a Xenon-Quartz lamp fadeometer. An obvious change resulted but it was not clear whether this was due to fading of the Prussian blue or merely chalking. In any case, there were not obvious differences in the ME spectrum of the two halves of the panel. It is not certain at this time that a change could be detected if the blue on the surface had faded because in the transmission configuration a spectrum results from the underlying, presumably unaffected, pigment. Therefore, this initial experiment was inconclusive.

For an experiment now underway, we have prepared Prussian blue using enriched ^{57}Fe so that much thinner paint films can be used. We have also prepared separate samples with ^{57}Fe in the ferrocyanide ligand only and in the ferric ions only. These panels are now in the fadeometer. Spectrophotometric measurements of reflected light will be compared before and after fading and ME spectra will be obtained by scattering.

2.3 EFFECT OF PARTICLE SIZE ON ME SPECTRA. — As mentioned above, there is evidence that one of the

important properties effecting the color as well as the ME spectrum obtained from a sample of pigment is the size of the particles. A number of workers have reported this phenomenon [8] as an example of superparamagnetism. To help examine this hypothesis, we first obtained X-ray diffraction patterns for four materials to ascertain whether the FeOOH in each case was of the α-, β-, γ- or δ-variety (or mixtures of these). Of these four samples, B-103 (a synthetic lemon yellow oxide), B-22 (a yellow ochre), B-28 (a raw turkey umber), and B-65 (cappagh brown), none showed any evidence of the presence of anything but α-FeOOH, yet the ME spectra of these four, in the order given here, showed less and less of the 6-peak spectrum normally expected for α-FeOOH.

Subsequently, electron micrographs were taken of these samples and one other (B-411, a raw sienna) and are shown in figures 9, 10, 11, 12, and 13 along with

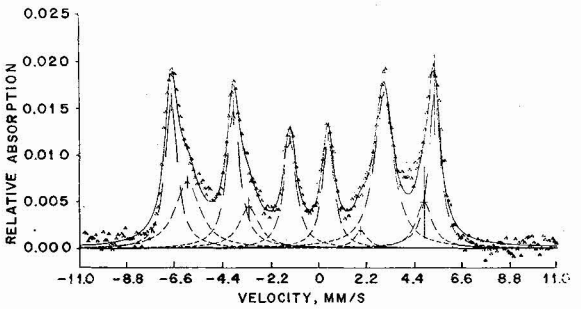

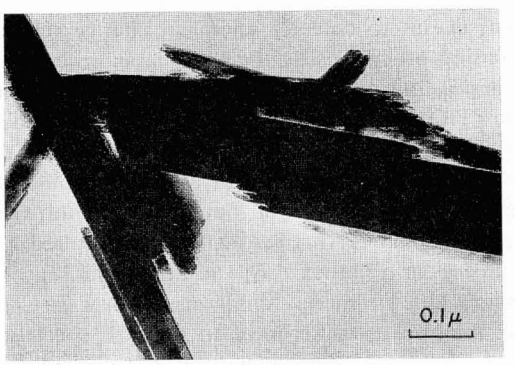

FIG. 9. — Lemon yellow oxide B-103.

the ME spectra obtained. The correlation between the particle size and the type of spectrum obtained is obvious. We, therefore, conclude that the spectra obtained for *natural* α-FeOOH-bearing pigments usually exhibit superparamagnetism while *synthetic* α-FeOOH does not. This is due mainly to the smaller particle size occurring in the natural materials. It also appears that some of this phenomenon may also be due to the presence of clay in the natural material. ME spectra of iron chemically bound to clay particles has been reported [11]. These spectra show slightly greater quadrupole splitting resulting in 2 peaks somewhat further apart than those obtained for superparamagnetic α-FeOOH. This may contribute to the total spectrum but the small differences in peak location and the low intensity defies their resolution.

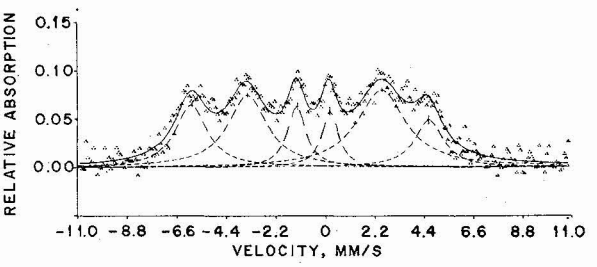

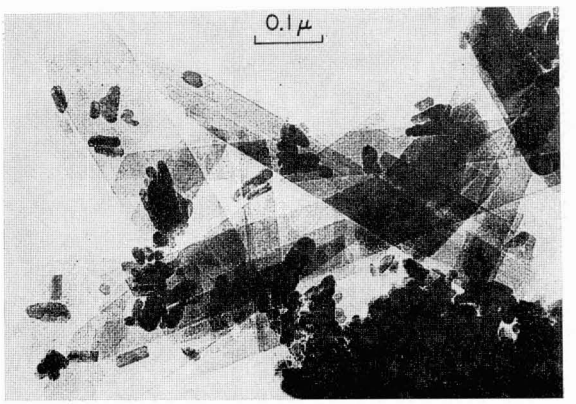

FIG. 10. — Raw sienna B-411.

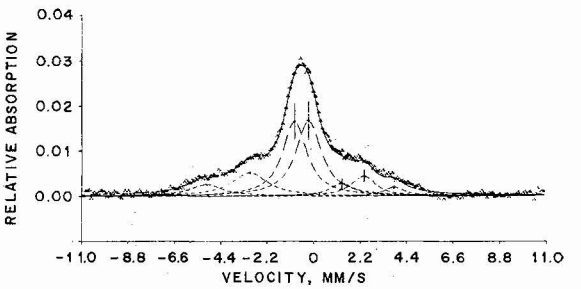

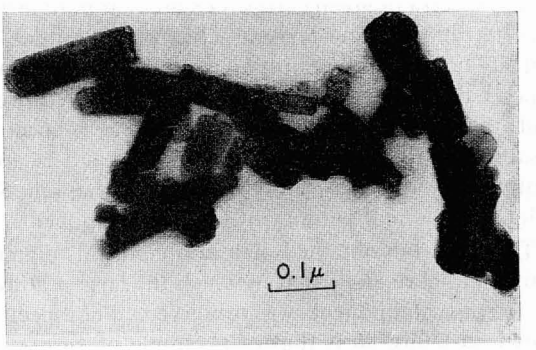

FIG. 11. — Yellow ochre B-22.

One may explain the unusual spectra obtained for some natural α-Fe_2O_3 on the basis of particle size and/or the presence of clay in a similar manner. Although it requires even smaller particles to produce

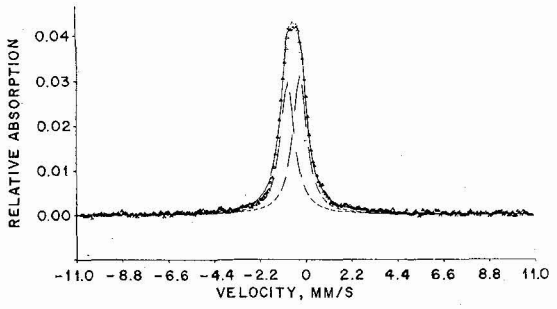

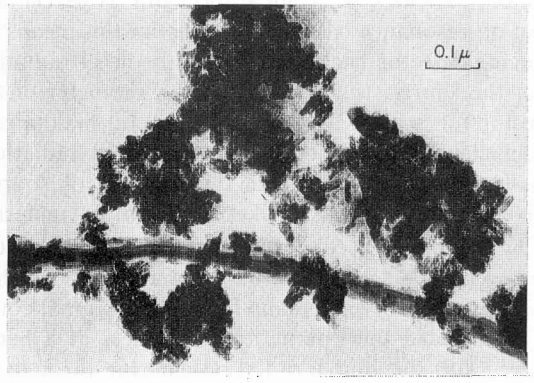

FIG. 12. — Raw turkey umber B-28.

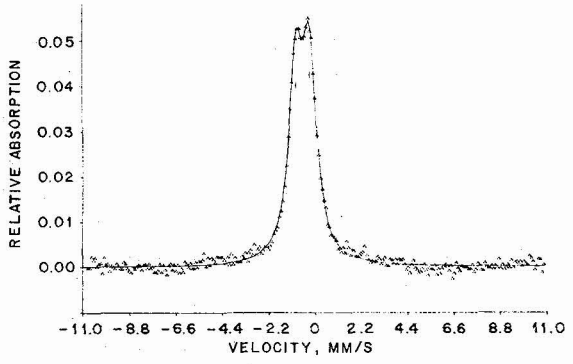

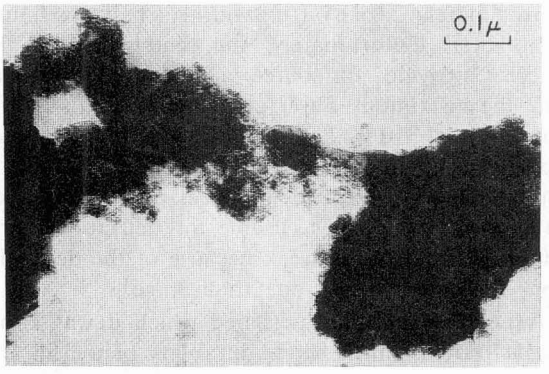

FIG. 13. — Cappagh brown B-65.

superparamagnetism in α-Fe_2O_3 (compared to α-FeOOH), this phenomenon has been reported [12]. A series of simple experiments confirmed this for the materials with which we are working.

Calcination of coarsely crystalline synthetic α-FeOOH (B-57) resulted in the expected 6-peak spectrum of α-Fe_2O_3 (1) while the same treatment of a typical yellow ochre (B-21) yielded, in addition to the 6-peak spectrum, two peaks in the center.

Since this could also be the result of the presence of clay in the ochre, a finely divided sample of α-FeOOH was prepared which exhibited an amorphous structure and a completely superparamagnetic ME spectrum. Calcination of this material to α-Fe_2O_3 yielded a product exhibiting a spectrum similar to that of calcined yellow ochre. In fact, the superparamagnetism of this synthetic α-Fe_2O_3 was even more apparent than that obtained from the calcined ochre. A second sample of α-FeOOH, which was slightly more crystalline (2), yielded ME spectra (for untreated and calcined material) that exhibited less superparamagnetism (see Fig. 14).

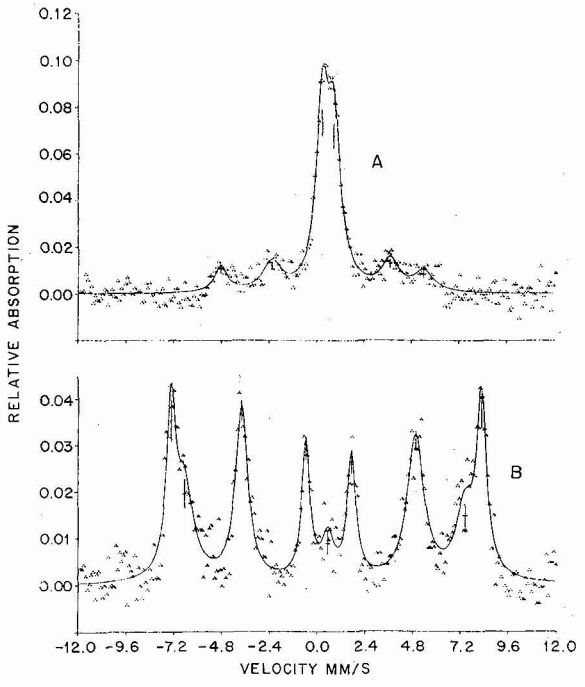

FIG. 14. — *a*) Synthetic α-FeOOH (small crystals). *b*) The same calcined to α-Fe_2O_3.

We conclude that natural red oxides are, as in the case of the yellow oxides, more finely divided than their synthetic counter-parts. There must also be some clay-bound iron oxide present because in a few samples, one could distinguish the wider spacing of the central peaks, typical of the spectra obtained for clay-iron oxide preparations [11].

2.4 DETERMINATION OF MIXTURES OF OXIDES. — Figure 6 is the spectrum obtained from a brown material prepared by mixing yellow iron oxide, red

(1) This and a few of the following results were obtained by ME scattering rather than by transmission.

(2) As shown by means of X-ray diffraction.

iron oxide, and carbon black. We wished to devise means of determining the relative quantities of the iron oxides in such mixtures and also in those containing the black oxide.

We prepared a range of mixtures of combinations of yellow-red, red-black, and black-yellow in known proportions and obtained ME spectra for these. In mixtures containing yellow oxide, there was no problem in resolving two superimposed spectra and correlating the relative peak intensity with the ratios. We found that ratios as small as 1 : 9 could be readily determined.

Mixtures of red and black oxides were not so easily resolved, especially when there was a large preponderance of one component over another. We found, however, that we could *ask* the computer to fit the most positive peaks of the superimposed spectra as if only one peak were present. The position of this peak varied with the composition of the mixture from 7.02 mm/s for pure Fe_3O_4 (black) to 7.60 mm/s for pure α-Fe_2O_3 (red) (velocities relative to our CoO source).

Unfortunately, our spectrometer control drive was not sufficiently reproducible in its settings to enable us to find a useful correlation. Later, when we were operating in the scattering mode, certain modifications did enable us to accomplish this.

Figure 15 shows the results we obtained in the scattering configuration using a chromium-Co-57

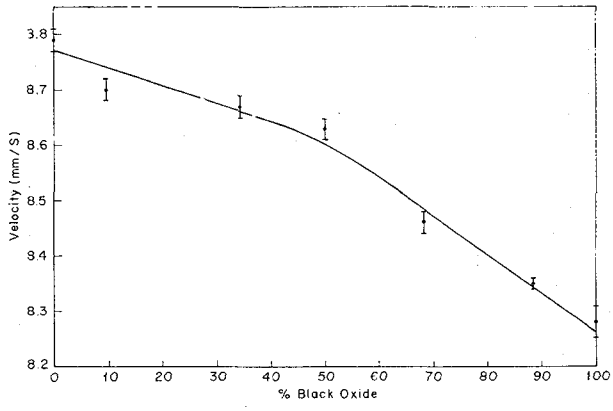

FIG. 15. — Mixtures of α-Fe_2O_3 and Fe_3O_4. Most positive peak velocity as a function of concentration.

source (see part 2.3). The utility of this means of determining the ratios of black and red oxides in mixtures is apparent from this figure. However, since particle size effects the position and widths of the peaks, this technique must be utilized with caution when the materials involved are natural oxides.

3. **Mössbauer effect by scattering.** — 3.1 APPARATUS AND EXPERIMENTAL ARRANGEMENT. — The key element in any attempt to obtain Mössbauer spectra in a scattering configuration is the radiation detector. A number of workers [1, 13] have published results obtained with various techniques. Our detector is based upon a design that originated with Chow *et al.* [1] with improvements suggested by Flinn [14] and certain modifications of our own. This detector, which has performed remarkably well, is described below. Throughout our experiments, the electronic equipment used was the same as that described above for our transmission work.

Naturally, one strives for a maximum *signal-to-noise* ratio which can be measured as a percent effect in a Mössbauer spectrum obtained with a specified sample material. Percent effect is here defined as the increase in count rate at a peak in a spectrum as percentage of an off-resonance base line. In practice this means (*a*) reducing detector background, mainly direct radiation from the source, (*b*) maximizing the geometry of the detector for scattered radiation, and (*c*) maximizing the efficiency of the detector for scattered radiation. Finally, one must maximize the fraction of source-derived radiation that strikes the sample material.

Chow *et al.* [1] used a configuration based upon the detection of 14 keV scattered γ-radiation in which a 90 % krypton-10 % methane-filled proportional counter surrounded the sample approximately as a hemisphere, with the source radiation entering through an opening in the apex of the hemisphere. The result was a toroidally-shaped detector with a center wire that forms an octagon within the toroid. The window that admitted the scattered radiation was aluminized polyethylene made as thin as possible to reduce losses due to adsorption. The energy resolution obtained was not very good, the 14 keV gammas being barely discernible as a separate peak.

Flinn [14], working to optimize this configuration, first suggested (*a*) thinner anode supports, (*b*) a guard to compensate for field distortion at the anode lead-in, (*c*) thinner window material of polypropylene and (*d*) a more perfect toroidal shape for the detector and a more circular shape for the anode. An attempt to follow these suggestions did provide a somewhat better detector with a resolution for 14.4 keV gamma rays of approximately 2.8 keV (full width of half maximum) at its best. Unfortunately, the center hole of this detector, provided for source radiation, was too small and the maximum observed Mössbauer Effect for stainless steel 310 was only approximately 15 percent. Additional source shielding and relocation of the source eventually yielded an effect of approximately 20 to 25 %. While this was usable, this detector required refilling at least every week because of the deterioration of the resolution due to leakage.

A new detector was designed which it was hoped would provide much better durability of the fill and, by use of a larger center hole, would also provide more efficient utilization of the source. No attempt was made to maintain the perfect toroidal shape of the earlier detector and circular shape of the anode.

A major change was that of the window material. A brief literature search revealed that polypropylene allows the diffusion of oxygen at a rate consistent with

our observations on time-dependent deterioration of detector performance [15]. Nylon, on the other hand, was known to exhibit diffusion rates approximately 140 times smaller than polyolefins. An aluminized nylon window was, therefore, incorporated in the new design at first. This was thinner than the previously used polypropylene which tends to compensate for the increased average atomic number of the nylon. Unfortunately, while nylon provides an excellent barrier against oxygen, water is not effectively barred. Therefore, we eventually used a machined beryllium window.

Figure 16 shows sectional views of the detector. All seals to the body of the detector were made with a

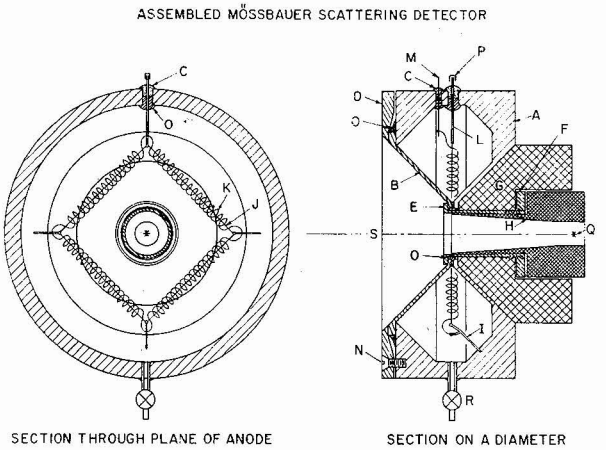

FIG. 16. — Cross-section views of Mössbauer Scattering Detector. *a*) Detector body (Aluminum) ; *b*) Window (Beryllium, .035″ thick) ; *c*) Epoxy seal ; *d*) Clamping plate (Aluminum) ; *e*) Clamping sleeve (Aluminium) ; *f*) Clamping sleeve nut (Brass) ; *g*) Shielding (Tungsten) ; *h*) Collimator (Tungsten) ; *i*) Quartz support (one of three, 2 mm diam.) ; *j*) Anode (.001″ diam. wire) ; *k*) Grid (.020″ diam. wire) ; *l*) Anode lead (hypodermic needle tubing) ; *m*) Grid lead ; *n*) Clamping plate bolt (one of eight) ; *o*) High vacuum epoxy seal ; *p*) Soldered cap ; *q*) Source position ; *r*) High vacuum valve ; *s*) Typical sample position.

commercially available ([3]) epoxy resin, especially formulated for high vacuum work. The detector cavity consists only of cylindrical or conical surfaces to eliminate any need to machine the compound curve necessary to achieve a true torus. The anode-guard system is that first used by Flinn. The anode, .001″ diameter Neutraloy ([4]), is supported by three one mm diameter quartz rods cemented into holes in the detector body and a tubular lead-in made of hypodermic needle tubing. (These quartz supports were actually doubled to form supports for the guard.) The anode is thus shaped in a square.

An epoxy seal of special design forms the insulating feed-through for the anode. A second epoxy seal provides the seal for the lead to the guard. The guard itself is made of tantalum wire formed into a spiral shape with longitudinal members to form a complete envelope for the anode.

Tungsten shielding was used in the most critical areas.

The performance of this detector has been outstanding. The operating voltage is 1 000 V with the guard grid at approximately 300 V. When freshly filled with a mixture of 90 % krypton-10 % methane ([5]) the resolution for 14.4 keV gamma rays is approximately 1.8 keV (full width at half maximum) as shown in figure 17. A Mössbauer Effect spectrum taken with .001″ thick Stainless Steel (Type 302, approximately 70 % Fe, natural) as a sample yields an effect of over 400 percent and a linewidth (fwhm) of 0.44 mm/s as shown in figure 18. The effective sample area with the geometry used here is approximately 5 cm^2. The data to which the computer fitted the curve in the figure

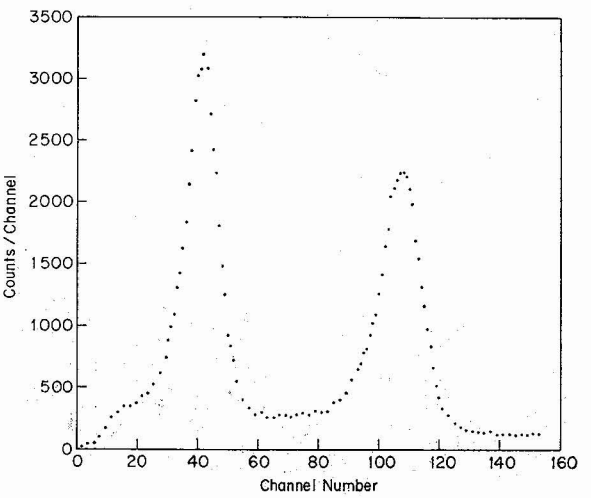

FIG. 17. — Response of detector to radiation from ^{57}Co.

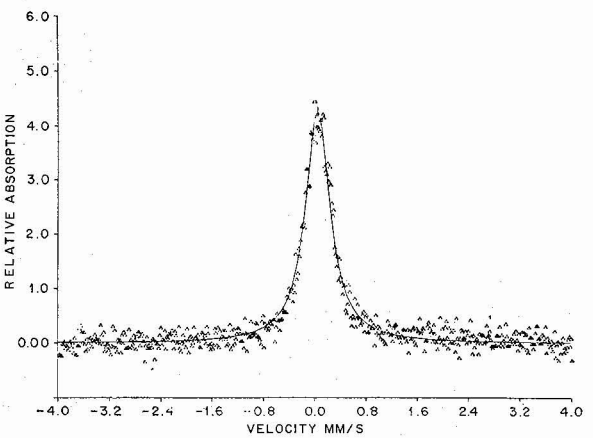

FIG. 18. — Scattering spectrum. Stainless Steel 302 (Natural).

([3]) Veeco, Inc., Plainview, N. Y.
([4]) Mole-cue Wire Company, Wall Township, N. J.

([5]) Research grade supplied by Matheson Gas Products, East Rutherford, N. J. The filling system incorporates an oil diffusion pump to attain the best possible removal of air (oxygen) from the detector prior to filling.

was obtained in approximately one hour with a 30 mc. ^{57}Co source (in chromium). The data acquisition rate, off resonance, was approximately 2 000 c/hr/channel (256 channels). After all small leaks were sealed the detector was filled and no degradation in performance was noted for a period of 18 months.

3.2 BULK PIGMENTS BY SCATTERING. — Several typical pigments were analysed by scattering for comparison with the data obtained for the same materials by transmission. These samples were loosely packed with a 1/32″ deep Plexiglas(R) holder approximately 7/8″ in diameter and covered with a 2 mil polyethylene film. The spectrometer drive was calibrated with natural iron. (Note that not all of the following results were obtained with the new detector under optimal conditions ; many of these were obtained while the detector was still under development.)

The results obtained by scattering of Sample B-375 (red iron oxide), B-57 (yellow iron oxide), B-367 (black iron oxide), and B-21 (yellow ochre), were compared with the results which were obtained by transmission and showed, as expected, the equivalence of the two methods of measurement.

3.3 NON-DESTRUCTIVE MÖSSBAUER SPECTRA OF PIGMENTS IN PAINTINGS. — Figure 19 shows the set-up for obtaining a Mössbauer spectrum of the iron-

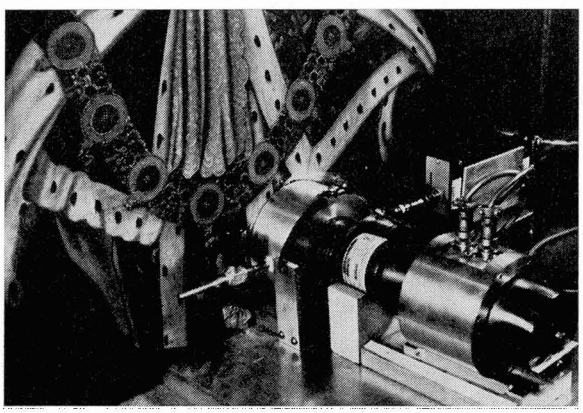

FIG. 19. — Mössbauer effect spectrometry of an 18th century painting.

bearing pigments in a 18th century painting. (At the time, we were limited to an area of the painting within approximately 9 cm of the edge of the work. However, we have now rearranged the base of the system so that any point on the surface of a painting within 45 cm of the edge is accessible for this analysis.) In the figure, the part of the painting undergoing analysis is a light-brown decorative detail on the subject's cape. The resulting spectrum, shown in figure 20, is typical for a natural yellow-ochre. Figures 21 and 22 show spectra of the dark backgrounds of two other maintings from the 18th century. The former appears to be typical of natural red ochres while the latter is typical of a raw umber.

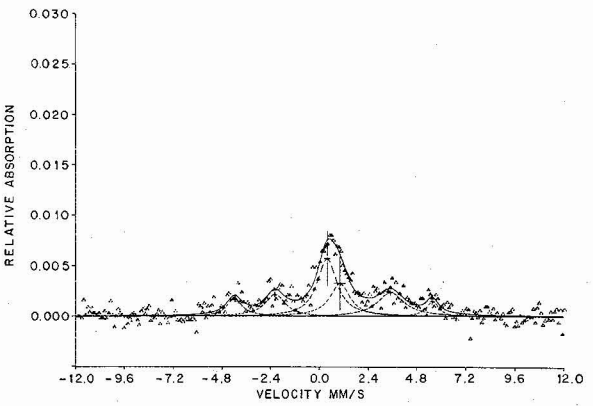

FIG. 20. — Light brown area of painting in figure 19.

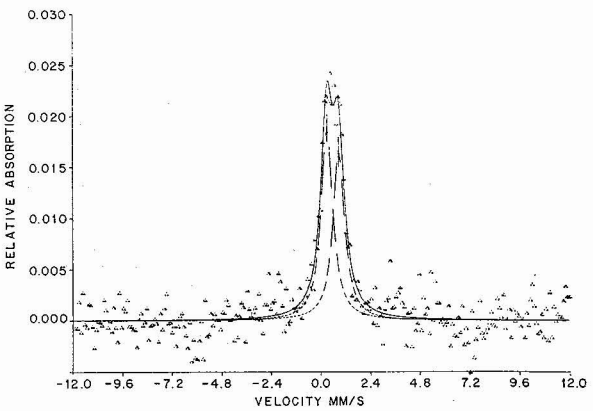

FIG. 21. — Dark Background of an 18th century painting.

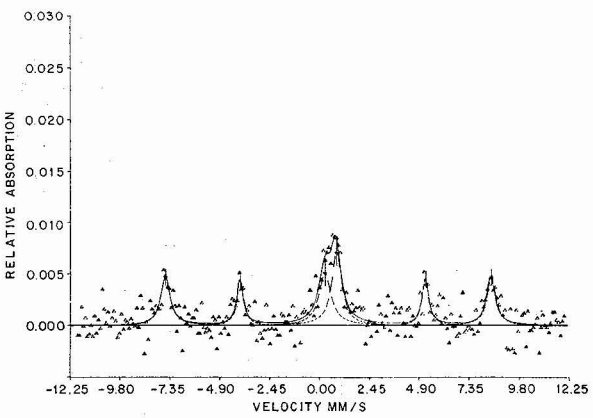

FIG. 22. — Dark Background of an 18th century painting.

Each of these spectra were obtained over a period of 2 to 3 days although, with the detector optimized, one day would probably be sufficient.

The use of this technique as an aid to solving problems in identification would involve the study of several works by an artist (or school) to which an unknown work is attributed. While this would not permit one to make a positive identification, it could provide strong corroboration with absolutely no harm to the works involved.

3.4 MÖSSBAUER SPECTRA OF IRON IN TERRACOTTA STATUARY. — 3.4.1 *General.* — The color of terracotta is mainly due to the presence of iron in the material. Using neutron activation analysis, we found concentrations of iron ranging from 2.3 to 21 percent with a mean of approximately 6 percent. Most of our samples were sufficient to provide either a chunk measuring 1/2 to 1 inch across or a powder sample to fill our 1/32 inch deep sample holder. We undertook to obtain ME spectra, by scattering, to determine if there were differences which might lead to a means of identification. We also investigated the effect of heating some of these to temperatures high enough to change their color and the chemical state of the iron in them.

Samples from 24 terracotta works were analysed. Several of these were taken from different places on a given piece so that the total number of spectra obtained was approximately 32, not including experiments involving additional heating of the terracotta. Not all of the works were believed genuine. Among those that were beyond suspicion we generally found that one of two *types* of Mössbauer spectra were obtained. These are illustrated in figures 23*a* (TC-3) and 23*b* (TC-19).

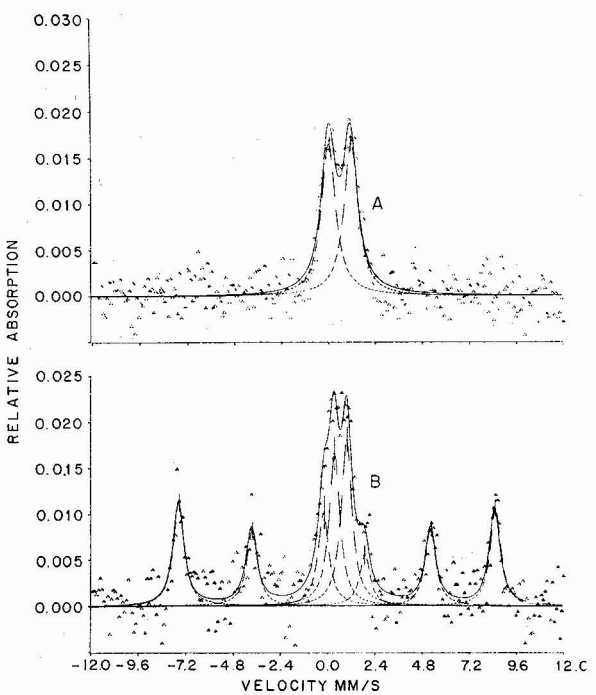

FIG. 23. — *a*) Terracotta, TC-3. *b*) Terracotta, TC-19.

The spectrum shown for sample TC-3 shows virtually no magnetic hyperfine splitting and is not unlike that obtained for a clay-iron complex by other workers [11]. Sample TC-19 appears to be a mixture of at least two components, α-Fe_2O_3 and another, nonmagnetic, material. It is noteworthy that the two-peak spectrum of this latter component is not the same as that obtained from sample TC-3. In nearly every well-authenticated case, one or the other of the spectra appeared (i. e. two peaks separated by approximately 0.8 to approximately 1.1 mm/s *or* superimposed spectra of α-Fe_2O_3 and a component yielding 2-peaks with a separation of $\sim$ 0.5 to $\sim$ 0.8 mm/s). In a few cases, a four-peak spectrum was obtained. The latter, however, was predominately like that obtained for sample TC-3.

In a few instances, where two or three works were known to be by the same artist, very similar spectra were obtained. The use of this technique appears to offer useful corroboration of authenticity pending the acquisition of a larger collection of data.

3.4.2 *Effect of baking temperature.* — When we first encountered TC-3-type of spectrum, the question arose whether this represented clay that had not been heated to *normal* temperatures for baking terracotta. Therefore, an experiment was initiated using sample TC-4, which consisted of heating the sample to successively higher temperatures with Mössbauer spectra taken after each heat. Figure 24 shows some of the results obtained ([6]).

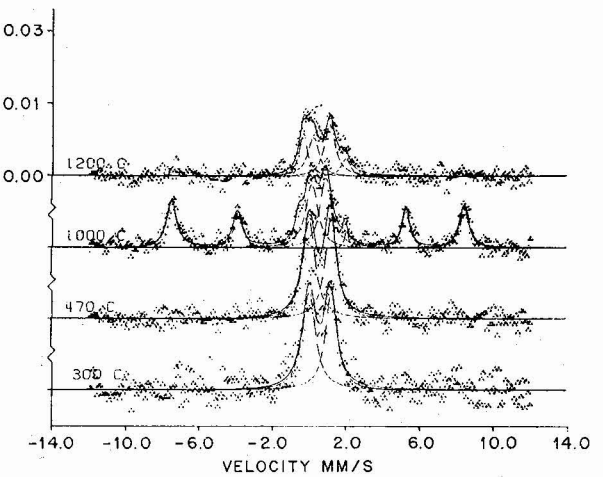

FIG. 24. — Terracotta, TC-4, after heating to various temperatures.

The spectrum obtained at room temperature was not changed by heating to a temperature of 770 °C (the curve for 770° is not shown). After heating at 1 000 °C, we noted a deepening of the color as well as the change of the Mössbauer spectrum from a typical TC-3-type to a TC-19-type. Finally, at 1 200 °C, the sample melted to a brownish, glassy solid which, of course, would not ever be observed in a museum piece.

With the tentative assumption that the observance of the TC-19-type spectrum indicates a higher firing temperature, we noted several other relationships in our data. First, those pieces yielding TC-19-type

([6]) Indicated temperature are only approximate as the furnace controls were not calibrated.

spectra were more *modern* than those that did not (for example, late 16th century as opposed to early 15th), indicating that perhaps better temperature control was obtainable by the later period. Note, however, that many of the later productions also yielded TC-3-type spectra.

Second, on one large piece, samples of different colors were taken from different parts. These samples yielded slightly different spectra, with those that were lighter corresponding to a TC-3-type spectrum and those that were darker showing more of the TC-19-type. Subsequent heating of the lighter samples to $\sim$ 1 000 °C produced material which was similar, in both color and spectra obtained, to the darker samples.

It would appear that certain artists and craftsmen were more skilled in the management of their furnaces and thus produced a more evenly fired work and at a higher temperature than others. Evaluation of whether or not this results in a higher quality product is beyond the present scope of this project ; we merely indicate that these differences occur.

To further investigate the change that occurs at higher baking temperatures, a clay was obtained that appears to be similar to that used by artists for terracotta. In experiments presently underway, this phenomenon will be explored not only as a function of temperature but also of other conditions such as rate and time of heating.

3.4.3 *The identification of fakes.* — A small number of works of highly dubious authenticity were also included in our survey. We have been able to make some tentative conclusions that may help classify some of them. While all superficially appear to be terracotta, a closer look at the chemical and physical properties of the material indicated that some are not. Apparently good imitations of terracotta are produced by a cement-like material homogeneously colored to look genuine. Unfortunately, with only small samples available, it requires some painstaking effort to reveal such differences by microscopy or chemical analysis. Mössbauer spectra obtained from such materials, however, appear to be rather different than those obtained from genuine works. Usually these imitation terracottas yield a spectrum much like that shown in figure 4*a*, which is a finely divided (amorphous) α-FeOOH. This could indicate either that a very fine natural pigment (umber ?) was mixed into the material before shaping or that α-FeOOH was actually precipitated in the wet mixture.

Another type of forgery that we have tentatively identified involves mismatching of the materials of works that presumably should be identical. For example, out of one unified group of three figures, two were analysed by Mössbauer Effect scattering. One of these, not necessarily genuine but believed to be of greater age, yielded a TC-3-type spectrum. The second yielded a TC-19-type spectrum. The distinction was quite clear-cut and suggests that they were not produced at the same time by the same artist.

A second suspect piece, TC-9, was attributed to an artist of which two genuine samples (TC-18 and TC-19) were available. While the latter two showed distinct TC-19-type spectra, the suspect work yielded a TC-3-type spectrum. Tentatively one is tempted to rule out the attribution of the suspect work. This conclusion also was reinforced by trace element analysis obtained by neutron activation.

A demonstration of the effectiveness of the scattering mode was provided by showing that an extremely well matched but pieced-on arm of a figure was made of a different material than the rest. This showed that the arm was not only a repair but a replacement produced at a later date. The *mis-matched* spectra were obtained without any sampling whatever.

At this point in our survey of terracottas, one can safely conclude that a valuable tool is at hand. However, as in much of this type of work, a much larger body of data is necessary to ascertain the reliability of determinations such as those tentatively made here.

References

[1] CHOW, H. K. *et al.*, *Mössbauer Effect Spectrometry for Analysis of Iron Compounds*, U. S. Atomic Energy Commission Report No. NSEC-4023-1 (October 1969).

[2] HARLEY, R. D., *Artists' Pigments, c.* 1600-1835 (Butterworths, London) 1970.

[3] GETTENS, R. J. and STOUT, G. L., *Painting Materials* (Dover, New York) 1966.

[4] SAWATZKY, G. A. *et al.*, *Phys. Rev.* **183** (1969) 383.

[5] BERNAL, J. D. *et al.*, *Clay Minerals Bull.* **4** (1959) 15-30.

[6] ASTM Standards 1958, Part 8, pp. 58-63, Amer. Soc. for Testing Materials, Philadelphia (1959).

[7] Reference [2] p. 156.

[8] SHINJO, T., *J. Phys. Soc. Japan* **21** (1966) 917-922 ; VAN DER KRANN, A. M. and VAN LOEF, J. J., *Phys. Lett.* **20** (1966) 614-616.

[9] KELLEY, W. H. *et al.*, *Phys. Rev.* **124** (1961) 80.

[10] GRISSOM, C., MA Thesis, Oberlin College, O. (1974).

[11] YASSOGLOU, N. J. and PETERSON, J. B., *Soil Science Soc. Amer. Proc.* **33** (1969) 967-970.

[12] KÜNDIG, W. and HANS BÖMMEL, *Phys. Rev.* **142** (1966) 327-333.

[13] KOCH, R. C. *et al.*, *Mössbauer Spectrometry for Analysis of Iron Compounds*, U. S. Atomic Energy Commission Report No. NSEC-4010-1 (1967) ; TERRELL, J. H. and SPIJKERMAN, J. J., *Appl. Phys. Lett.* **13** (1968) 11-13 ; ORD, R. N., *Appl. Phys. Lett.* **15** (1969) 279-281.

[14] FLINN, P. A. and O'CONNELL, T., U. S. Atomic Energy Commission, Report WASH-1220 (1973).

[15] STANNETT, V. *et al.*, *Permeability of Plastic Films and Coated Paper to Gases and Vapors*, TAPPI Monograph Series No. 23, Technical Association of the Pulp and Paper Industry, New York, 1962, pp. 12-27.